

# Dust accretion and destruction in galaxy groups and clusters

Sean L. McGee<sup>1</sup>\* and Michael L. Balogh<sup>1</sup>

<sup>1</sup>*Department of Physics and Astronomy, University of Waterloo, Waterloo, Ontario, N2L 3G1, Canada*

30 October 2018

## ABSTRACT

We examine the dust distribution around a sample of 70,000 low redshift galaxy groups and clusters derived from the Sloan Digital Sky Survey. By correlating spectroscopically identified background quasars with the galaxy groups we obtain the relative colour excess due to dust reddening. We present a significant detection of dust out to a clustercentric distance of 30 Mpc/h in all four independent SDSS colours, consistent with the expectations of weak lensing masses of similar mass halos and excess galaxy counts. The wavelength dependence of this colour excess is consistent with the expectations of a Milky Way dust law with  $R_V=3.1$ . Further, we find that the halo mass dependence of the dust content is much smaller than would be expected by a simple scaling, implying that the dust-to-gas ratio of the most massive clusters ( $\sim 10^{14} h^{-1} M_\odot$ ) is  $\sim 3\%$  of the local ISM value, while in small groups ( $\sim 10^{12.7} h^{-1} M_\odot$ ) it is  $\sim 55\%$  of the local ISM value. We also find that the dust must have a covering fraction on the order of 10 % to explain the observed color differences, which means the dust is not just confined to the most massive galaxies. Comparing the dust profile with the excess galaxy profile, we find that the implied dust-to-galaxy ratio falls significantly towards the group or cluster center. This has a significant halo mass dependence, such that the more massive groups and clusters show a stronger reduction. This suggests that either dust is destroyed by thermal sputtering of the dust grains by the hot, dense gas or the intrinsic dust production is reduced in these galaxies.

**Key words:** galaxies: evolution, galaxies: formation, galaxies: structure

## 1 INTRODUCTION

Dust grains have long been known to play an important role in the interstellar medium and the star formation which occurs within a galaxy. Further, because dust grains can absorb and redden background sources, an accurate knowledge of the large scale distribution of these grains is crucial. Groups and clusters of galaxies present a unique opportunity to study this large scale distribution as well as the processes important in dust evolution. Dust within massive clusters is thought to sputter on timescales of  $10^7$  -  $10^9$  years (Draine & Salpeter 1979), depending on the density and temperatures of the environment. This is caused by the ejection of atoms from the dust grain by the collision with sufficiently energetic gas particles. Given the presence of a distributed, hot plasma in groups and clusters, the short timescale for sputtering means that dust observed in these systems must have been accreted recently. This potentially gives a probe of the relevant dust creation processes.

Recently Ménard et al. (2009b) have shown that dust excesses exist out to Mpc scales around  $i < 21$  galaxies. There are a variety of mechanisms by which dust may escape from galaxies and become distributed on such large scales. Star-forming galaxies are often seen to have large outflows of gas and dust which are blown

out by the power from supernova feedback (Heckman et al. 1990; Tremonti et al. 2007). In addition, active galactic nuclei (AGN) can have significant power, and the jets they induce may be able to remove gas and dust from galaxies and redistribute it within the larger environment (e.g. McNamara & Nulsen 2007). During galaxy-galaxy mergers a significant amount of the gas and dust may be removed due to collisional processes, or subsequently blown out by the induced star-formation or AGN power (Hopkins et al. 2006). Observations of galaxies falling into massive clusters show gas and dust being stripped from the galaxy and incorporated into the surrounding environments (Crowl et al. 2005; Domainko et al. 2006).

The temperatures and densities of the large scale environments of groups and clusters are difficult to probe observationally. While X-ray observatories have allowed the determination of the temperatures and densities of massive clusters to near the virial radius (e.g. Vikhlinin et al. 2005), analysis of the detailed properties of representative samples of groups has largely relied on stacking large samples (Dai et al. 2007) and/or been limited to measuring total X-ray luminosities (Rykoff et al. 2008). As a result, the densities and temperatures of the environments outside the virial radius are largely inferred from simulations alone (Pfrommer et al. 2006; Kay et al. 2007). Indeed, the non-detection of significant amounts of baryonic material in the local universe has given rise to the postulate that this material is contained in overdense gas with tem-

\* Email: s2mcgee@uwaterloo.ca

peratures of  $10^5$ - $10^7$ , dubbed the warm-hot intergalactic medium (WHIM) (see Bregman 2007). The expected temperature and density of the WHIM are likely able to destroy dust through thermal sputtering. Therefore, measuring the large scale dust distribution is a potentially powerful probe of the large scale temperatures and densities.

Previous attempts to measure the dust centered on clusters has focused on the inner regions, largely within the virial radius. Observations of typical groups ( $< 10^{13.5} h^{-1} M_{\odot}$ ) have not yet been done. The first attempts to quantify the dust content of clusters involved the counting of relative deficiency of background sources. These attempts generally agreed that the  $V$ -band attenuation is on the order of 0.2-0.4 (Zwicky 1951; Bogart & Wagoner 1973; Boyle et al. 1988; Romani & Maoz 1992). However, early infrared observations of clusters attempting to detect direct emission from this dust largely led to non or marginal detections, implying dust masses much lower than that implied by background counts (Annis & Jewitt 1993; Wise et al. 1993; Stickel et al. 2002; Montier & Giard 2005). Similarly, recent observations with Spitzer have also failed to show dust masses implied by 0.2-0.4 magnitudes of attenuation (Bai et al. 2007).

Recently, large, uniform surveys have made detecting statistical colour excesses of background sources of large samples of clusters feasible. Chelouche et al. (2007) have correlated background quasars with intervening galaxy clusters and found that, for massive clusters, the excess reddening,  $E(B-V)$ , is on the order of 0.004 magnitudes in the central Mpc. Bovy et al. (2008), using the spectra of early type galaxies, found an upper limit on the extinction within 2 Mpc of massive clusters to be  $A_V < 0.003$  magnitudes. Similar results were obtained by Muller et al. (2008), who found, using photometric redshifts to identify background galaxies, a similar result of  $A_V = 0.004 \pm 0.010$  mag of attenuation. However, these type of measurements are differential measurements and, as such, are dependent on the control sample of sources with which the colour excess is measured. Since it is known that clusters of this halo mass have significant excess mass out to at least  $20 h^{-1}$  Mpc (Sheldon et al. 2007b), and indeed Chelouche et al. (2007) has shown that the colour excess varies at least out to 5 Mpc from the cluster center, then the presence of dust on these larger scales may bias the measurement of the central regions.

In this paper, by measuring the reddening effect on background quasars, we examine the large scale ( $\sim 50 h^{-1}$  Mpc) radial profile of dust centered on groups and clusters. This is the first measurement of such large scales and the first to probe such low mass groups. The large scale is important to separate the cluster/group dust from the dust expected to be associated with individual galaxies. We discuss the data in §2 and present the method and the measurement in §3. We discuss the implications of the measurement in §4 and summarize our findings in §5. Throughout this paper, we adopt, as was done during the assembly of the group catalogue, a  $\Lambda$ CDM cosmology with the parameters of the third year WMAP data, namely  $\Omega_m = 0.238$ ,  $\Omega_{\Lambda} = 0.762$ ,  $\Omega_b = 0.042$ ,  $n = 0.951$ ,  $h = H_0/(100 \text{ km s}^{-1} \text{ Mpc}^{-1}) = 0.73$  and  $\sigma_8 = 0.75$  (Spergel et al. 2007).

## 2 DATA

The technique we use to examine the dust content of galaxy groups and clusters is conceptually simple. Our approach relies on measuring the change in the mean colour of background sources as a function of their projected distance from groups and clusters. It is

expected that the change in the mean colour will be small, and thus we must stack the signal from many clusters together to measure the effect on the distribution of background sources. Therefore, we require a large sample of groups and clusters, which are uniformly selected and have well defined masses. We also require that we have a large number of background sources with an intrinsic colour distribution with little scatter and which do not vary with sky position. The background sources must also be at high redshift, so that they are not physically associated with the clusters we are examining. For these purposes, the best publicly available data is derived from the the Fourth Data Release (DR4) of the Sloan Digital Sky Survey, a five colour ( $ugriz$ ) photometric and spectroscopic survey covering over  $4780 \text{ deg}^2$  and containing  $\sim 670,000$  spectra of galaxies, quasars and stars (Adelman-McCarthy et al. 2006). Below we discuss the group sample and the sample of background objects drawn from this survey which are used in this paper.

### 2.1 Galaxy group catalogue

The majority of galaxies in the local universe reside in some kind of association with at least one other galaxy (Eke et al. 2004). However, quantifying the mass of a large sample of those associations is difficult. In particular, X-ray temperature or luminosity, often used as a mass indicator in galaxy clusters (Reiprich & Böhringer 2002), is too low or faint in galaxy groups to determine mass for a survey the size of the SDSS. Also, the velocity dispersions of galaxies, which are often used as tracers of the potential well of clusters or massive groups, is ineffective when the groups contain only a handful of spectroscopically confirmed galaxies. Recently, Yang et al. (2005) showed that an effective mass estimate of galaxy groups can be obtained by essentially ranking groups by their total luminosity and associating these rankings with the expectations of a  $\Lambda$ CDM halo occupation model.

Yang et al. (2007) have applied their algorithm to the SDSS DR4 to produce a sample of  $\sim 300,000$  galaxy groups with masses as low as  $10^{11.5} h^{-1} M_{\odot}$ . In this paper we use “Sample I” from Yang et al. (2007), which exclusively uses galaxies with SDSS spectroscopic redshifts. We chose this sample, as opposed to the other samples, which add in existing redshifts from the literature, because we are principally concerned with obtaining a uniformly selected population of galaxy groups. In the most recent galaxy group catalogue of Yang et al., the authors rank the galaxy groups both by total luminosity in the  $r$ -band as well as the total stellar mass of the group. In this paper, we will use the group masses obtained by the ranking the total stellar mass, with the goal of minimizing the effect of a particular group’s recent star formation history. However, we note that because we must stack many groups in relatively wide mass bins, this choice has no effect on the results. Finally, we restrict our analysis to galaxy groups with masses greater than  $10^{12.5} h^{-1} M_{\odot}$ , which leaves a final sample of 75947 groups between  $z=0$  and  $z=0.2$ . Figure 1 shows the halo mass distribution of our group sample broken into three mass bins which we use later in the paper.

### 2.2 Background objects: spectroscopically identified quasars

Our principal concerns when choosing a sample of background objects to examine are that the sources are at sufficiently high redshift that they are not physically associated with the group, that they represent a relatively uniform population, with a small dispersion about their average properties, and that their colours

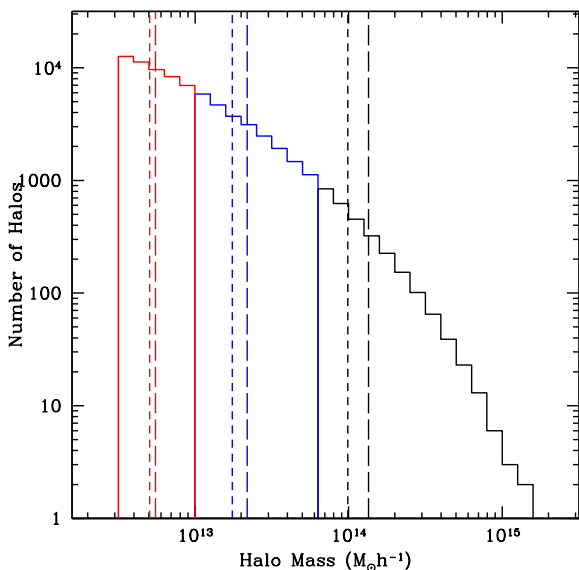


**Figure 1.** The halo mass distribution of the galaxy group and cluster sample. The sample is shown in three groups of halo mass, from  $10^{12.5}$  to  $10^{13} h^{-1} M_{\odot}$  (red),  $10^{13}$  to  $10^{13.8} h^{-1} M_{\odot}$  (blue), and  $10^{13.8}$  to  $10^{15.3} h^{-1} M_{\odot}$  (black). The short dashed (long dashed) line in each bin represents the median (mean) halo mass of the bin.

are well calibrated. For all these reasons we have chosen to examine the photometric properties of spectroscopically identified quasars drawn from the fourth edition of the SDSS quasar catalog (Schneider et al. 2007). This catalog contains  $\sim 77,000$  quasars brighter than  $M_i = -22$  drawn from the fifth SDSS data release, and are targeted based on their photometric properties and/or the presence of an unresolved radio source (Richards & others. 2002). We reduce this sample to contain only quasars within DR4, ie. those for which we have an identified group sample. The SDSS quasar catalog contains *psf* magnitudes for each of the five bands of SDSS photometry (*ugriz*), with typical errors of 0.03 mag. The colours have been corrected for galactic extinction using the dust maps of Schlegel et al. (1998). We only examine quasars with redshifts between  $z = 1$  and  $z = 3$  in order to avoid quasars physically associated with the target groups, or extreme objects at high redshift.

### 3 ANALYSIS

Our first goal is to measure the change in the mean colour of the background quasars as a function of their position from foreground clusters. This change in the mean colour is also known as the excess reddening because interstellar dust is observed to extinguish light more readily at the blue end of visible light, causing the light to redder.

We parametrize the excess reddening,  $E(i - j)$ , of a source,  $k$ , as

$$E(i - j)^k = m_i^k - m_j^k - \langle m_i - m_j \rangle_{control} \quad (1)$$

where  $m_i$  and  $m_j$  are the magnitudes in the  $i$  and  $j$  bands of the source for which the excess reddening is measured. The final term in this expression is the mean colour of the control sample of objects. In practise, the excess reddening measured in this way of a single background source is dominated by the intrinsic distribution

width of colours of that source. However, with the assumption that the background sources have a well defined mean colour we can stack large numbers of sources to measure a mean excess colour,  $\langle E(i - j) \rangle$ . Therefore, by stacking many background sources in bins of projected distance,  $r$ , from the centre of our group and cluster samples, we can obtain an excess colour profile of the groups and clusters,  $\langle E(i - j) \rangle(r)$ .

A key feature of this type of measurement is the control sample of sources. Unless the unobscured mean colour of the background sources is known, it must be made as a differential measurement with respect to a control sample of background sources. In the literature, the control sample is not well defined. Bovy et al. (2008) use a control sample of all background sources greater than  $2 h^{-1}$  Mpc from the center of a cluster, while Chelouche et al. (2007) defines the control sample to be background sources which are greater than  $7R_{200}$  from the cluster center. We have, by trial and error, found that the differential dust signal approaches zero only at  $>40 h^{-1}$  Mpc from the center of the cluster. So, the control sample of background sources is must be taken from large radius. The control sample of quasars are defined as those which have projected clustercentric distances,  $r$ , of  $46 h^{-1}$  Mpc  $< r < 50 h^{-1}$  Mpc from a given cluster in the sample.

Notice that, similar to the weak lensing or cluster correlation measures, our dust measurement is a correlation measurement. A given quasar can have a small projected distance from cluster A, but still be counted as a control quasar if it is in the control range of cluster B. In other words, each quasar is in many clustercentric radial bins. Because of the much larger area covered by the control sample of quasars, the number of quasars in the control sample greatly outnumber the number of quasars in any of the other samples. This enables us to do a Monte Carlo estimation of the error in the excess colour by selecting 200 independent samples of control quasars which have the same number as a given target bin. The error bars are then the 1 sigma limits of the excess color from the 200 trials for each bin.

### 3.1 Large scale distribution

We begin by examining the total colour excess from a stacked set of all the groups in our sample. We measure the mean colour of the background quasars within clustercentric annuli in projected radius bins of  $2 h^{-1}$  Mpc, out to  $50 h^{-1}$  Mpc from the cluster center. The five band photometry of the SDSS quasar sample allows for the measurement of four independent excess reddening signals. Figure 2 shows the colour excess for each of the four sets of independent colours.

As Figure 2 shows, a significant colour excess is measured in all four independent colours as far out as  $30 h^{-1}$  Mpc from the group and cluster centre. The typical projected virial radius of a group or cluster of this mass ( $M \sim 10^{13.5} h^{-1} M_{\odot}$ ) is only  $\sim 1 h^{-1}$  Mpc. Thus, such a significant large scale distribution of reddening is initially surprising. However, studies of the cluster correlation function (Bahcall & Soneira 1983), and the weak lensing profile of similar clusters (Sheldon et al. 2007b; Johnston et al. 2007) shows that there is a significant excess of matter out to similar distances from clusters. We expect that the dust excess to such large scales is just a result of this excess matter, although we will address this further in §4.2.

While the size of the measured excess reddening shown in Figure 2 is quite small ( $< 0.015$  mag), if it is due to the presence of dust then it corresponds to a large and extended dust distribution. However, there are some systematic effects which must be accounted

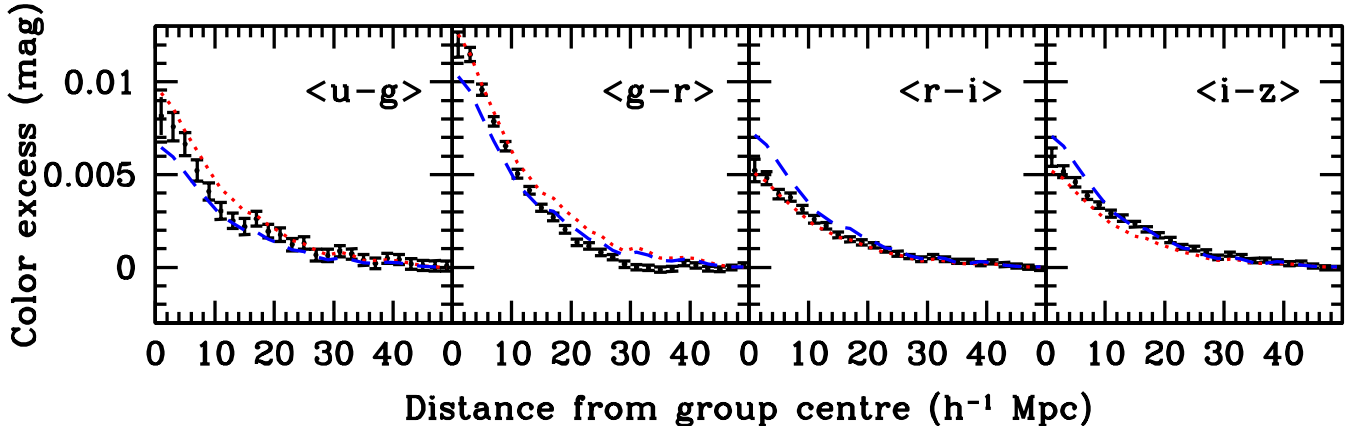


**Figure 2.** The excess colour of four independent colours as a function of distance from the group center. The excess colour is measured with respect to the colour of quasars at a projected distance of 46 to 50  $h^{-1}$  Mpc. The error bars are 1 sigma errors from Monte Carlo estimation. The blue, dashed line (red, dotted line) represents the  $R_V=2.0(5.0)$  dust reddening law which minimizes the chi-square for  $A_V$  as a function of radius.

for before we can be sure the reddening is due to dust. In particular, galaxy groups and clusters have significant mass, and therefore sources behind this mass will be gravitationally magnified. A sample of sources which is chosen by a fixed flux limit will lead to more high redshift sources, and a lower absolute luminosity limit at fixed redshift behind the cluster, than for a patch of sky far from the cluster. Thus this measurement is potentially affected when the intrinsic mean colour of the background sources is luminosity or redshift dependent.

We can estimate the size of the magnification effect of our groups and clusters. We would expect this effect to trace the mass distribution, so it would be most pronounced close to the cluster. Johnston et al. (2007) measured the mass profile of a large sample of galaxy clusters and found that at a distance of 1  $h^{-1}$  Mpc from the most massive clusters the surface mass density is  $\sim 10^2 h M_\odot/\text{pc}^2$ . This corresponds to a magnification of  $\sim 0.02$  magnitudes — a minute change in the effective limiting magnitude of our quasar sample. Given this, we see that for our  $\langle g-r \rangle$  measurement of  $\sim 0.011$  at 1  $h^{-1}$  Mpc to be completely explained by magnification of a quasar sample with varying mean colour, the intrinsic *cumulative*  $g - r$  colour of our quasar sample would have to vary by 0.55 per magnitude near the magnitude limit. However, we find that the cumulative  $g - r$  colour of the control sample of quasars only varies by 0.005 magnitudes from  $i=19$  to  $i=20.2$ , the magnitude limit of our sample. In other words, as it is for all four independent colours, the size of the magnification-induced reddening effect is two orders of magnitude smaller than required to explain our results.

We note that the possibility of having foreground emission from the group or cluster contribute to the the reddening signal is not physical, given that the local background subtraction used in the quasar photometry will remove this component.

### 3.2 Wavelength dependence of reddening

Here we consider the wavelength dependence of the reddening, to gain some indication of the nature of the dust. The wavelength dependence,  $R_V$  is commonly parametrized by linking the absolute extinction in the  $V$  band,  $A_V$  to the excess  $B - V$  colour as

$$R_V = \frac{A_V}{E(B - V)}. \quad (2)$$

A value of  $R_V = 3.1$  is generally used based on studies of interstellar Milky Way dust, but values in the range from 2.5 to 5 have been measured for the Magellanic clouds (Prevot et al. 1984) and starbursting galaxies (Calzetti et al. 2000). In contrast, the emission from a typical collection of cluster galaxies would have a negative  $R_V$ . Unfortunately, we can not directly determine  $R_V$  because we do not have  $B$  and  $V$  magnitudes. However, using the fitting functions of O'Donnell (1994), we can transform our excess colours to determine  $A_V$  and to determine whether the shape of the expected reddening curve is consistent with the known properties of interstellar dust.

In Figure 2, we also show the predictions of two dust reddening laws, one with  $R_V = 2.0$  and one with  $R_V=5.0$ . To do this we must find the  $A_V$  value at each radial bin from the combination of the four independent colours. We do this by minimizing the chi square value at each step given the errors on each colour. For the majority of the colours and radii, these two dust laws essentially bracket the data. This seems to suggest that the colour profile is very similar to that expected from known dust laws. However, we would like to make a more precise measurement, which we do by stacking the data in radial bins.

In Figure 3, we show the reddening of background quasars in two radial bins for each photometric band with respect to the  $r$  band. The solid black line in each panel is the extinction curve expected from an interstellar dust law with  $R_V=3.1$ . The dust attenuation,  $A_V$ , is 0.0223 in the panel showing the inner  $10 h^{-1}$  Mpc, while it is 0.0097 for the  $10 > r > 20 h^{-1}$  Mpc bin. While the  $R_V=3.1$  law shows reasonable agreement with the wavelength dependence of the reddening, we also allow  $R_V$  to be fit simultaneously with  $A_V$ . These results are shown with the dotted line and correspond to best fitting  $R_V$  values of 3.3 and 3.5 in the two radial bins respectively. Thus, the reddening is very similar to the expectations of a Milky Way dust law.

### 3.3 Halo mass dependence

We now explore how this dust distribution depends on the mass of the host halo. In Figure 4 we show the qso  $\langle g-i \rangle$  colour excess as a function of distance from the group center in three bins of total group mass. The  $\langle g-i \rangle$  colour is chosen as our principle measure of the dust reddening in the remainder of the paper. These two photometric bands are the best calibrated, and have been recently used

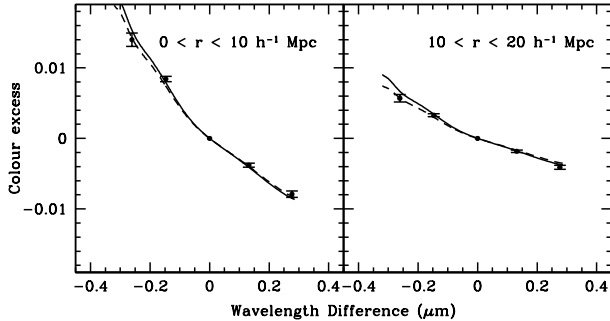


**Figure 3.** The colour excess in two bins of radial distance from the group centres. The solid black line is the expectations from a  $R_V=3.1$  dust law, using the expansion of (O'Donnell 1994), with a attenuation of  $A_V = 0.0223$  and 0.0097 for the  $0 > r > 10 h^{-1}$  Mpc and  $10 > r > 20 h^{-1}$  Mpc bins respectively. The dotted line is the result of simultaneously fitting for  $R_V$  and  $A_V$ , which results in  $(R_V, A_V) = (3.3, 0.0220)$  and  $(3.5, 0.0094)$  in the two radial bins, respectively. The data points are for the colours u-r, g-r, r-r, i-r, z-r respectively.

in the literature. Conveniently, the  $\langle g-i \rangle$  is most closely related to the more commonly used  $B-V$  dust colour as (Prevot et al. 1984; Ménard et al. 2008)

$$E(g-i) = \frac{\lambda_g^{-1.2} - \lambda_i^{-1.2}}{\lambda_B^{-1.2} - \lambda_V^{-1.2}} E(B-V) \quad (3)$$

$$= 1.55 E(B-V). \quad (4)$$

Using this transformation, and assuming  $R_V=3.1$ , we show the corresponding dust attenuation in the  $V$  band,  $A_V$ , on the right ordinate axis. Quite strikingly we see that the centers of the clusters have dust attenuations of  $A_V \sim 0.03$ -0.04, when measured with respect to quasars  $\sim 45 h^{-1}$  Mpc away. In comparison, the disk of a spiral galaxy at a similar redshift has a dust attenuation of  $A_V \sim 0.25$  mag (Holwerda et al. 2009). This suggests that the dust signal cannot be localized to disks within the line of sight alone, because the covering fraction of such group and cluster members is much less than  $(0.03/0.25) = 0.12$ . In other words, there must be a significant component of dust which is not localized within the disks of  $\sim 0.1 L^*$  galaxies alone. A similar conclusion was reached recently by Ménard et al. (2009b), who showed that the dust attenuation around galaxies extends well beyond the radius expected if the dust was confined to the disk. We examine this further in §3.4.

It is also noticeable that the dust distribution shows a relatively small halo-mass dependence, in that the most massive bin shows a larger colour excess than the lowest mass bin at each position out to  $20 h^{-1}$  Mpc. However, except at the inner most bins, the measured colour excess in each of the three mass bins is always within  $\sim 0.001$ -0.002 magnitudes, a much smaller range than the range of their values as a function of group centric distance. A possible explanation for such a small dependence on the halo mass could be that the halo masses themselves are uncertain, so that perhaps the wide halo mass bins actually contain roughly the same size groups. However, it is worth noting that the fraction of red galaxies within these same groups show a significant halo mass dependence. 50% of the  $L_*$  galaxies in  $10^{14} h^{-1} M_\odot$  are “early type” while only 20% of the same galaxies are “early type” in  $10^{12.5} h^{-1} M_\odot$  haloes (Weinmann et al. 2006). This argues that the masses are well defined for a statistical study such as this.

In the bottom panel of Figure 4, we show the same  $\langle g-i \rangle$  colour excess but now as a function of scaled radius, namely  $R_{180}$ .

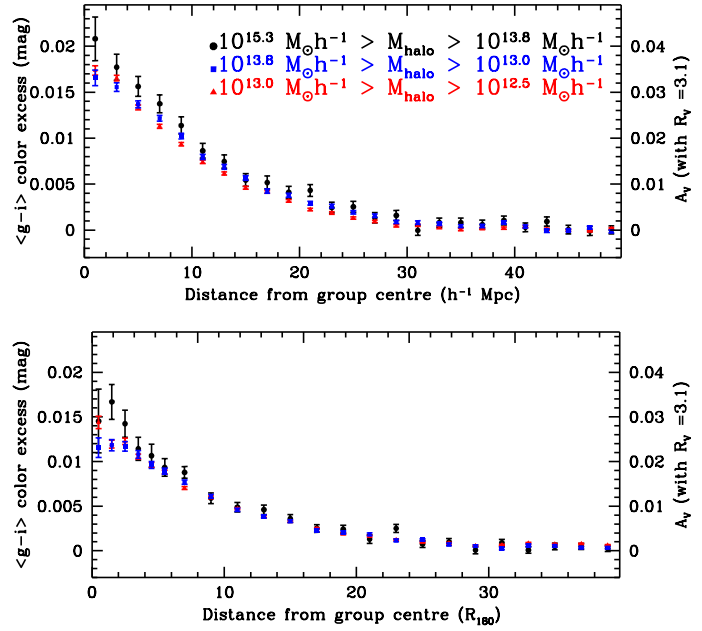


**Figure 4.** The  $g - i$  colour excess in three samples of galaxy groups as a function of distance from the group center. The  $V$  band attenuation  $A_V$  is plotted on the right ordinate axis assuming  $R_V=3.1$ . This is shown as a function of physical distance (top panel) and in  $R_{180}$  (bottom panel).

For this plot we have used the individual  $R_{180}$  of each cluster, rather than using the median  $R_{180}$  of each bin. This is an important point, as simply scaling physical distance in the top panel by the median  $R_{180}$  would result in lower mass groups actually have a higher reddening than higher mass groups. However, because there is a range of  $R_{180}$  in each bin, the result is to almost completely remove the halo mass dependence, especially at distances far from the cluster. It appears that the dust reddening is similar at a given scaled radius far from the cluster. We will return to the interesting behavior at small scales in §4.2.

### 3.4 Spatial distribution of the dust

By measuring the quasar colour excess as the difference in the mean value of the quasars, our results are insensitive to the spatial distribution of the dust. If the dust exists in concentrated clumps with a small covering fraction, then the colour excess could be driven by relatively few objects with large reddening values. However, if the dust is uniformly distributed we would expect each quasar to be reddened by the mean value.

In an attempt to address this question, we explore the color excess as a function of the percentiles of the quasar color distributions. In order to determine what fraction of quasars contribute to the signal, we sort the quasars in a particular radial bin and those in the “control” background sample by their measured  $g-i$  colours. We bin each sample by percentile and measure the mean  $g-i$  colour in that percentile bin, and then subtract the measured mean  $g-i$  percentile colour of the cluster quasars from the measure mean  $g-i$  colour of the “control” sample for in the corresponding percentile. This leaves us with the  $\langle g - i \rangle$  colour excess in percentile bins.

Admittedly, this measure is difficult to interpret physically, so we first attempt to develop a framework in which to interpret the results by using simulated reddening on background quasars. We take as our control sample of quasars those which are the control

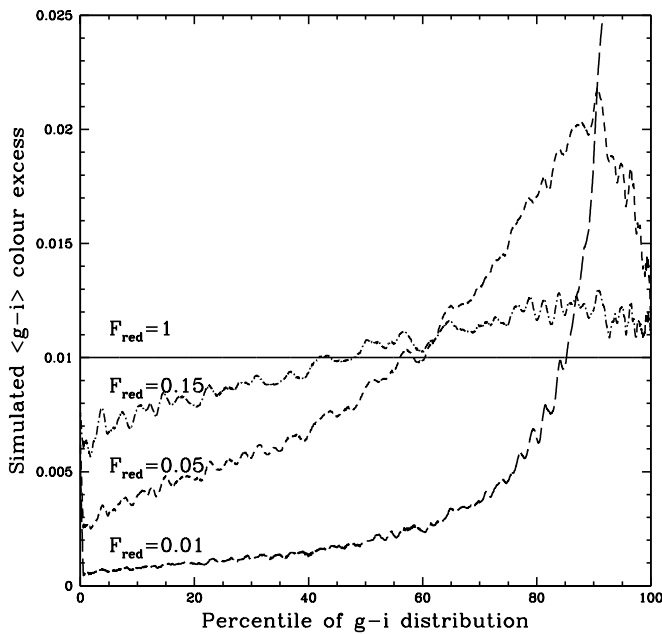


**Figure 5.** The simulated  $g - i$  colour excess as a function of percentile for four different reddening models. The model is set to have a mean color excess of 0.01 and  $F_{red}$  determines the fraction of objects which are reddened.

sample of the  $10^{13.5}$ - $10^{13}$  mass bin. We then add an amount of reddening to some fraction of the background quasars ( $F_{red}$ ) such that the mean colour excess is 0.01; for instance, all quasars can be reddened by 0.01 magnitudes, or 1/3 of the quasars can be reddened by 0.03 magnitudes. The results are shown in Figure 5, where  $F_{red}$  is varied to be 1, 0.15, 0.05 and 0.01. As expected, the color excess as a function of color percentile is flat for  $F_{red}=1$  and becomes more dominated by a high percentile peak with lowered  $F_{red}$ .

We now present Figure 6, which shows the color excess as a function of the percentiles of the real quasar color distributions. This is shown for several radial bins and for each halo mass range. We notice that for the majority of the radial bins the quasar color excess is relatively constant, never more than  $\sim 50\%$  away from the mean value in that bin. Comparing these with the results of our simulated data suggest that  $\sim 15\%$  of the quasars are causing this signal. Further, we see that the color excess curves become progressively steeper with decreasing radius, implying that the bulk of the signal is coming from fewer objects as we get near to the cluster. In the inner-most bin the reddening can be explained with 5–15% of the quasars dominating the signal.

As we will see in section §4.1, there are  $\sim 20$  galaxies ( $i < 21$ ) in the central  $2 h^{-1}$  Mpc of our most massive clusters. Thus, assuming that the reddening signal is concentrated uniformly in “bubbles” around these galaxies, a 10% covering fraction requires the “bubbles” to have radii of  $\sim 140 h^{-1}$  kpc. These bubbles are significantly larger than the typical size of the stellar mass in a galaxy (Shen et al. 2003; McGee et al. 2008). So, while this excess dust is not isotropically distributed throughout the groups, it also is not confined to massive galaxies.

The results of Figure 6 are also relevant in understanding a possible selection effect on our results. Our colour excess measurement are based on samples from a magnitude limited survey, and thus dust extinction may move quasars out of our sample, thereby

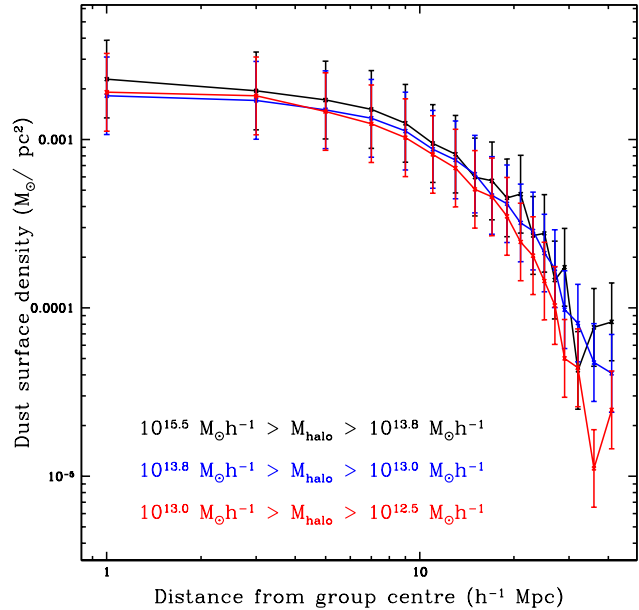


**Figure 7.** The excess dust surface mass density, in units of  $h M_{\odot}/pc^2$ , as a function of group-centric distance. This is shown for three different bins of group mass.

leaving a relatively reduced color excess. However, examining Figure 6 we see that there does not exist any significant population of highly extinguished quasars. Further, this result exists even when the sample is reduced to different magnitude bins. The lack of a highly extinguished population suggests that this is not a significant effect for the bulk properties of the sample.

#### 4 DISCUSSION

We have shown that there is a significant distribution of dust centered on galaxy groups and clusters and, in this section, we would like to measure some of its physical properties. This requires more information about the physical nature of the dust and, while we were able to show that the reddening is consistent with that expected from local interstellar dust, our measurements are somewhat crude. In what follows we will therefore make the assumption that the dust is similar to Milky Way interstellar dust with an  $R_V=3.1$ .

We are most interested in converting the  $A_V$  values we have measured into a dust mass surface density. To do this we need an estimate of  $K_{ext}$ , the extinction cross section for a given mass of dust:

$$\Sigma M_{dust} = \frac{A_V}{K_{ext}} \quad (5)$$

For this, we use the carbonaceous-silicate dust grain model developed by Weingartner & Draine (2001) and Li & Draine (2001) and subsequently tweaked by Draine (2003). These models have been shown to successfully reproduced the observed infrared emission, scattering properties and extinction properties of local interstellar dust. The value of  $K_{ext}$  is wavelength dependent, but in the  $V$  band it is  $K_{ext} = 1.54 \times 10^4 cm^2/g$ . With this assumption we can now directly show the surface mass density of dust which is responsible for the reddening signal. We plot this in Figure 7 for each of the three halo mass bins.

From this we conclude that the dust mass located within  $1 h^{-1}$  Mpc of the cluster center is on the order of  $10^{10} h^{-1} M_{\odot}$ ,

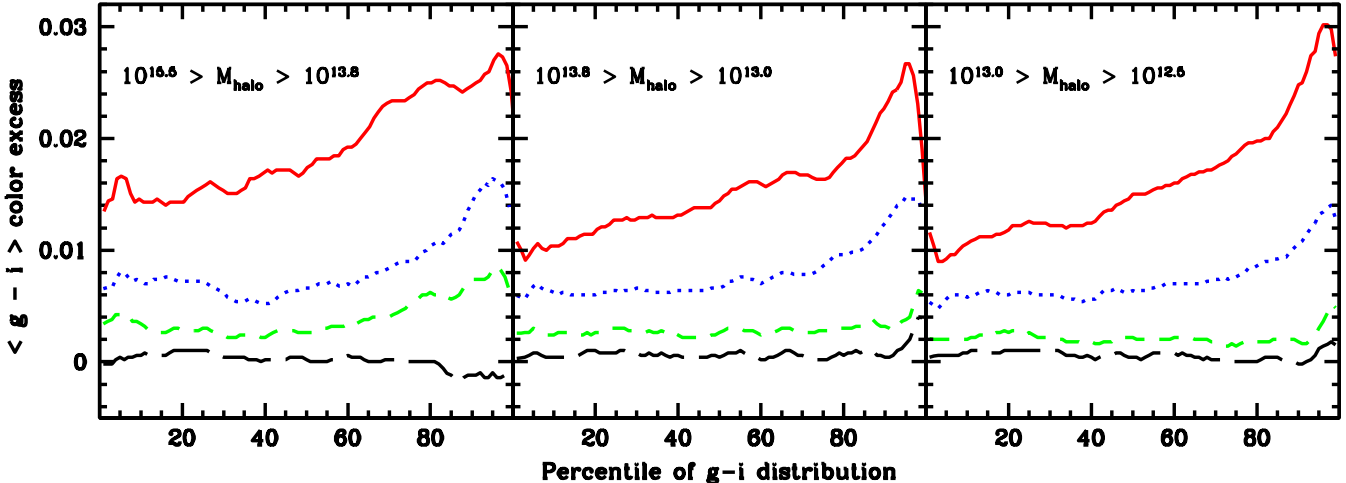


**Figure 6.** The relative color excess at a given percentile of the quasar color distribution. This is shown in several radial bins for each halo mass range. The color excess is measured with respect to the color at a given percentile of the control quasars. The red, solid line is for quasars within the central  $2 h^{-1} \text{ Mpc}$ , while the blue, dotted line is for quasars within  $9 < r (h^{-1} \text{ Mpc}) < 11$ . The green, dashed (black, long dashed) line is for quasars within  $19 < r (h^{-1} \text{ Mpc}) < 21$  ( $29 < r (h^{-1} \text{ Mpc}) < 31$ ).

with little dependence on halo mass. If we assume that the gas fractions of these clusters are equal to the universal baryon fraction this implies that, for a  $10^{14} h^{-1} M_{\odot}$  cluster, the dust-to-gas ratio is  $\sim 0.0003$ , or 3% of the interstellar medium ratio (Pei 1992). However, for a  $10^{12.5} h^{-1} M_{\odot}$  group, the ratio is  $\sim 0.0055$ , approximately 50% of the interstellar medium ratio.

Here it is worth examining the theoretical expectations of thermal sputtering. Draine & Salpeter (1979) have shown that, for dust grains principally composed of graphite, silicate or iron, collisions with gas of  $10^6 < T < 10^9$  K can destroy them. Then, for gas of this temperature dust grains can have a typical lifetime  $\tau$  of

$$\tau \approx 2 \times 10^4 \text{ yr} \left( \frac{\text{cm}^{-3}}{n_H} \right) \left( \frac{a}{0.01 \mu\text{m}} \right) \quad (6)$$

where  $n_H$  is the gas density and  $a$  is the radius of the typical dust grain. For the more massive clusters, a typical gas density is a few  $10^{-3} \text{ cm}^{-3}$  while interstellar grains are smaller than  $0.5 \mu\text{m}$  (Mathis et al. 1977). Therefore, dust grains in this gas will only survive for  $\sim 1$  Gyr. So any dust which exists in the more massive clusters must have been accreted within the last Gyr. McGee et al. (2009) have shown, using semi-analytic merger trees, that local galaxy clusters accrete  $\sim 5\%$  of their final galaxies per Gyr from otherwise isolated halos. This suggests that only 5% of the total accreted dust should exist in massive clusters today. This is remarkably similar to the implied dust-to-gas ratio of the most massive clusters.

#### 4.1 Excess galaxy profile

Ménard et al. (2009b) have recently shown that the dust-to-total mass ratio is approximately constant to a distance of 10 Mpc from individual galaxies. Similarly, they have shown that the dust-to-galaxy ratio is constant, except within the inner 20 kpc of the galaxy, where it's expected the signal is due to the galactic disk. We would like to explore similar ratios as a function of group centric radii. Unfortunately, we do not have available weak lensing mass profiles for our groups and clusters. However, we are able to correlate the excess number of galaxies in the SDSS photometry

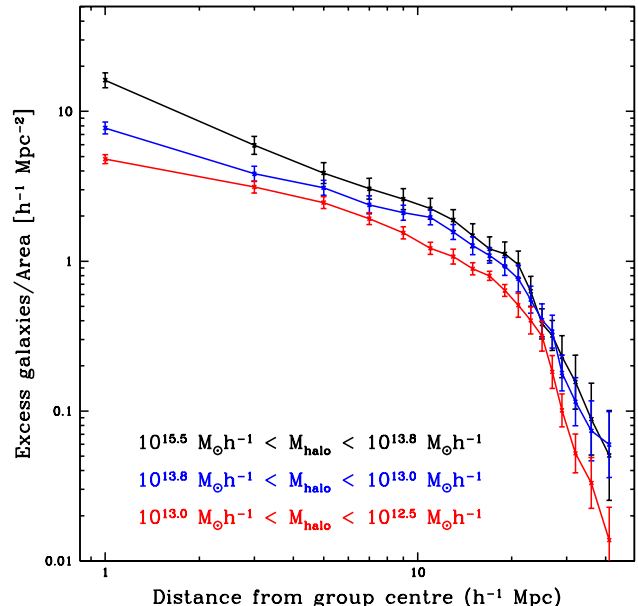


**Figure 8.** The excess number of galaxies ( $i < 21$ ) as a function of cluster-centric position for three bins of halo mass. The excess number was determined by statistical background subtraction. The uncertainties are 1 sigma expectations from the Jackknife method.

catalogues with the positions of our groups and clusters. Additionally, it is worth pointing out that Sheldon et al. (2007a) has found that, for clusters similar to ours, the weak lensing mass to light ratio is approximately constant from 1 Mpc to  $\sim 20$  Mpc. Therefore, we would expect that the galaxy/dust ratio should show similar trends to the mass/dust ratios.

In Figure 8, we present the excess number of galaxies as a function of cluster-centric position for each of the three bins of halo mass. This measurement was made by correlating the position of all SDSS galaxies with a galactic de-reddened  $i$  magnitude of  $< 21$ , where special care was taken with survey edges by using the

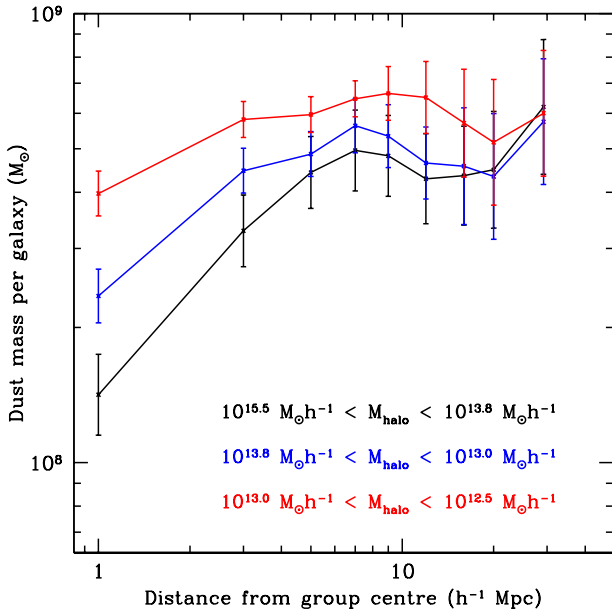


**Figure 9.** The excess surface dust mass per excess galaxy as a function of distance from the group centre.

SDSSpix code.<sup>1</sup> We choose to use the magnitude limit of  $i < 21$  because this limit was used by Ménard et al. (2009b). This figure demonstrates that the excess number of galaxies has a steeper slope in the inner  $10 h^{-1}$  Mpc than the similar excess dust mass plot. The figure also shows that there are significantly more galaxies in the higher halo mass bins, which again argues that the halo masses are well defined for large statistical samples.

#### 4.2 Dust mass associated with each galaxy

Now that we have compiled the excess dust mass distribution around the clusters and the excess galaxy number around the clusters, we can examine their ratio. We show this in Figure 9. There are a number of striking aspects of this plot. In particular, we see that for the bulk of the galaxies, those which are  $> 7 h^{-1}$  Mpc away, the excess dust mass per galaxy is on the order of  $10^9 M_\odot$ . This is approximately equal to the stellar mass of the median excess galaxy, and roughly agrees with supernova feedback models, which imply that up to 50% of metals produced are blown out of the galaxy (Finlator & Davé 2008). The constant dust per galaxy fraction also confirms our earlier suggestion that the dust excess seen out to large radii ( $> 30 h^{-1}$  Mpc) is simply due to excess halo clustering around galaxy groups and clusters.

However, the most obvious feature of this plot is the significant drop in dust mass per galaxy at small groupcentric radii, especially for the more massive cluster bin. The most massive clusters have dust to galaxy ratios  $\sim 15\%$  of the value far from the cluster, while small groups have  $\sim 80\%$  of the value. These numbers are not significantly different from the dust to gas ratios we found earlier.

There are two explanations for this reduction in the dust to galaxy ratio. First, as we have discussed, the dust could be destroyed by thermal sputtering in hot gas. Within a fixed physical radius, this sputtering would be more effective in clusters than in

groups, since the average density of the hot gas is substantially higher. Second, it is also possible that galaxies near clusters and groups may be fundamentally different in their dust creation properties. It is expected that most of the dust creation occurs in supernova, and it has been shown through extensive observations that groups and clusters have significantly lower star formation rates than isolated environments (Gómez et al. 2003; Balogh et al. 2004; Weinmann et al. 2006; Pasquali et al. 2009) and that difference extends to at least  $z=1$  (Wilman et al. 2005; Gerke et al. 2007; Balogh et al. 2009).

Unfortunately, the star formation rates in the large scale environments around groups and clusters have not been studied as extensively, especially at higher redshift. Lewis et al. (2002) have attempted to quantify this in the low redshift universe using a sample of massive clusters. They find that the mean star formation rate of galaxies is below the field value as far out as  $\sim 7$ -10 virial radii. Further, they see that the average star formation rate at 1 virial radius is 70% the isolated value. However, even despite this, the key to the amount of dust created is actually the stellar mass, which is essentially the integrated star formation rate. Since galaxy groups are actually quite efficient at producing stellar mass (Parker et al. 2005; Balogh et al. 2007), this suggests that the main driver of lower dust to galaxy ratios near clusters is not due to reduced dust creation. In effect, because the bulk of star formation/dust creation occurs at higher redshift the current cluster and field star formation rates are not as relevant.

#### 4.3 Impact on other science

We have shown that there is a significant and large scale variation in the dust reddening associated with galaxy groups and clusters. Although studying the properties of this dust and its implications for dust creation and destruction properties was the main goal of the paper, in this section we briefly assess the impact this reddening and attenuation of light might have on other studies.

Ménard et al. (2009a) have shown that not correcting for the impact of dust on background “standard candle” supernova can bias the measurement of  $\Omega_m$  at the few percent level. Here we point out an additional concern in the measuring of cosmological parameters. Our measurements imply that variations in attenuation by dust can be as high as 0.04 magnitudes in the  $V$  band (and higher in bluer bands). The next generation of large scale photometric surveys, such as LSST and DES, which principally are driven by the desire to probe the cosmological parameters, have design goals of 0.01 magnitude zeropoint stability from field to field (e.g. Ivezić et al. 2008; Tucker et al. 2007). Our measurements suggest this will not be possible to achieve without accounting for the dust in and around groups and clusters.

The dust attenuation may also be a problem for very low surface brightness features in clusters, such as the intra-cluster and -group medium. Zackrisson et al. (2009) have shown that because the dust extinguishes background light, measuring the sky background, of which the extragalactic background is a small part, some annulus from the cluster would lead to an over-subtraction. Crucially, this can lead to an underestimate of the intracluster light by as much as 1.3 magnitudes at an observed surface brightness of 30 magnitudes/arcsec<sup>2</sup> for attenuations of  $A_V=0.05$ . 30 magnitudes/arcsec<sup>2</sup> is close to the faint limit of the measurements of intracluster light by Zibetti et al. (2005). While an attenuation of  $A_V=0.05$  is not unreasonable given our results, as we have shown, the dust attenuation is dependent on the cluster-centric radius. Zibetti et al. (2005) et al. measured the sky background in a

<sup>1</sup> <http://dls.physics.ucdavis.edu/~scranton/SDSSpix/>

100-kpc thick ring with an inner radius of 1 Mpc centered on their clusters. Although this is below the spatial resolution of our measurements, we do note that our most massive cluster varies only from  $A_V \sim 0.042$  at 1  $h^{-1}$  Mpc to  $\sim 0.034$  at 3  $h^{-1}$  Mpc. In other words, we would expect that the variation in dust attenuations is not large ( $< 0.005$  mag), and therefore does not induce a significant underestimate in the intracluster light.

## 5 CONCLUSIONS

We have used a sample of spectroscopically identified high redshift quasars to probe the dust content of 70,000 uniformly selected galaxy groups and clusters. We have used the resulting colour excesses, in conjugation with synthetic dust models, to estimate the excess surface mass density around these clusters. Finally we have compared the resulting dust distribution with the excess galaxies around the same groups and clusters. Our findings are as follows.

- We have shown that there exists a large scale distribution of dust centered on groups and clusters with masses as low as  $M \sim 10^{12.5} h^{-1} M_\odot$ , and which extends 30  $h^{-1}$  Mpc from the group centre. The wavelength-dependence of this extinction is consistent with that expected for interstellar dust.
- We find that the dust must be distributed relatively uniformly, with a covering fraction on the order of 10 % to explain the excess color as a function of percentile of the color distribution.
- We find that the halo mass dependence of the dust content is much smaller than would be expected by a simple scaling, implying that the dust-to-gas ratio of the most massive clusters ( $\sim 10^{14} h^{-1} M_\odot$ ) is  $\sim 3\%$  of the local ISM value, while in small groups ( $\sim 10^{12.7} h^{-1} M_\odot$ ) it is  $\sim 55\%$  of the local ISM value.
- We find that the implied dust-to-galaxy ratio falls significantly closer to the group and cluster center. This reduction in the dust to galaxy ratio has a significant halo mass dependence, such that the more massive groups and clusters show a stronger reduction. This suggests that either dust is destroyed by thermal sputtering of the dust grains by the hot, dense gas or the intrinsic dust production is reduced in these galaxies.

## ACKNOWLEDGMENTS

We thank the referee, Stefano Zibetti, for suggestions which improved the paper. In particular, we thank him for clarifying the (non)-effect of foreground cluster emission. Further, we thank he and David Wilman for independent suggestions which led to Section 3.4. We also acknowledge useful conversations with Brice Ménard, David Gilbank, Mike Hudson, David Johnston, Clif Kirkpatrick and Carolyn McCoey. MLB acknowledges support from an NSERC Discovery Grant.

## REFERENCES

Adelman-McCarthy, J. K. et al. 2006, *ApJS*, 162, 38  
 Annis, J. & Jewitt, D. 1993, *MNRAS*, 264, 593  
 Bahcall, N. A. & Soneira, R. M. 1983, *ApJ*, 270, 20  
 Bai, L., Rieke, G. H., & Rieke, M. J. 2007, *ApJL*, 668, L5  
 Balogh, M., Eke, V., Miller, C., Lewis, I., Bower, R., Couch, W., Nichol, R., Bland-Hawthorn, J., Baldry, I. K., Baugh, C., Bridges, T., Cannon, R., Cole, S., Colless, M., Collins, C., Cross, N., Dalton, G., Driver, S. P., Efstathiou, G., Ellis, R. S., Frenk, C. S., N., Dalton, G., de Propris, R., Driver, S. P., Efstathiou, G., Ellis, R. S., Frenk, C. S., Glazebrook, K., Gomez, P., Gray, A., Hawkins, E., Jackson, C., Lahav, O., Lumsden, S., Maddox, S., Madgwick, D., Norberg, P., Peacock, J. A., Percival, W., Peterson, B. A., Sutherland, W., & Taylor, K. 2004, *MNRAS*, 348, 1355  
 Balogh, M. L., McGee, S. L., Wilman, D., Bower, R. G., Hau, G., Morris, S. L., Mulchaey, J. S., Oemler, Jr., A., Parker, L., & Gwyn, S. 2009, *MNRAS*, 398, 754  
 Balogh, M. L., Wilman, D., Henderson, R. D. E., Bower, R. G., Gilbank, D., Whitaker, R., Morris, S. L., Hau, G., Mulchaey, J. S., Oemler, A., & Carlberg, R. G. 2007, *MNRAS*, 374, 1169  
 Bogart, R. S. & Wagoner, R. V. 1973, *ApJ*, 181, 609  
 Bovy, J., Hogg, D. W., & Moustakas, J. 2008, *ApJ*, 688, 198  
 Boyle, B. J., Fong, R., & Shanks, T. 1988, *MNRAS*, 231, 897  
 Bregman, J. N. 2007, *ARA&A*, 45, 221  
 Calzetti, D., Armus, L., Bohlin, R. C., Kinney, A. L., Koornneef, J., & Storchi-Bergmann, T. 2000, *ApJ*, 533, 682  
 Chelouche, D., Koester, B. P., & Bowen, D. V. 2007, *ApJL*, 671, L97  
 Crowl, H. H., Kenney, J. D. P., van Gorkom, J. H., & Vollmer, B. 2005, *AJ*, 130, 65  
 Dai, X., Kochanek, C. S., & Morgan, N. D. 2007, *ApJ*, 658, 917  
 Domainko, W., Mair, M., Kapferer, W., van Kampen, E., Kronberger, T., Schindler, S., Kimeswenger, S., Ruffert, M., & Mangete, O. E. 2006, *A&A*, 452, 795  
 Draine, B. T. 2003, *ARA&A*, 41, 241  
 Draine, B. T. & Salpeter, E. E. 1979, *ApJ*, 231, 77  
 Eke, V. R., Baugh, C. M., Cole, S., Frenk, C. S., Norberg, P., Peacock, J. A., Baldry, I. K., Bland-Hawthorn, J., Bridges, T., Cannon, R., Colless, M., Collins, C., Couch, W., Dalton, G., de Propris, R., Driver, S. P., Efstathiou, G., Ellis, R. S., Glazebrook, K., Jackson, C., Lahav, O., Lewis, I., Lumsden, S., Maddox, S., Madgwick, D., Peterson, B. A., Sutherland, W., & Taylor, K. 2004, *MNRAS*, 348, 866  
 Finlator, K. & Davé, R. 2008, *MNRAS*, 385, 2181  
 Gerke, B. F., Newman, J. A., Faber, S. M., Cooper, M. C., Crotton, D. J., Davis, M., Willmer, C. N. A., Yan, R., Coil, A. L., Guhathakurta, P., Koo, D. C., & Weiner, B. J. 2007, *MNRAS*, 376, 1425  
 Gómez, P. L., Nichol, R. C., Miller, C. J., Balogh, M. L., Goto, T., Zabludoff, A. I., Romer, A. K., Bernardi, M., Sheth, R., Hopkins, A. M., Castander, F. J., Connolly, A. J., Schneider, D. P., Brinkmann, J., Lamb, D. Q., SubbaRao, M., & York, D. G. 2003, *ApJ*, 584, 210  
 Heckman, T. M., Armus, L., & Miley, G. K. 1990, *ApJS*, 74, 833  
 Holwerda, B. W., Keel, W. C., Williams, B., Dalcanton, J. J., & de Jong, R. S. 2009, *AJ*, 137, 3000  
 Hopkins, P. F., Hernquist, L., Cox, T. J., Di Matteo, T., Robertson, B., & Springel, V. 2006, *ApJS*, 163, 1  
 Ivezić, Z., Tyson, J. A., Allsman, R., Andrew, J., Angel, R., & for the LSST Collaboration. 2008, *ArXiv e-prints*  
 Johnston, D. E., Sheldon, E. S., Wechsler, R. H., Rozo, E., Koester, B. P., Frieman, J. A., McKay, T. A., Evrard, A. E., Becker, M. R., & Annis, J. 2007, *ArXiv e-prints*  
 Kay, S. T., da Silva, A. C., Aghanim, N., Blanchard, A., Liddle, A. R., Puget, J.-L., Sadat, R., & Thomas, P. A. 2007, *MNRAS*, 377, 317  
 Lewis, I., Balogh, M., De Propris, R., Couch, W., Bower, R., Offer, A., Bland-Hawthorn, J., Baldry, I. K., Baugh, C., Bridges, T., Cannon, R., Cole, S., Colless, M., Collins, C., Cross, N., Dalton, G., Driver, S. P., Efstathiou, G., Ellis, R. S., Frenk, C. S.,

Glazebrook, K., Hawkins, E., Jackson, C., Lahav, O., Lumsden, S., Maddox, S., Madgwick, D., Norberg, P., Peacock, J. A., Percival, W., Peterson, B. A., Sutherland, W., & Taylor, K. 2002, MNRAS, 334, 673

Li, A. & Draine, B. T. 2001, ApJ, 554, 778

Mathis, J. S., Rumpl, W., & Nordsieck, K. H. 1977, ApJ, 217, 425

McGee, S. L., Balogh, M. L., Bower, R. G., Font, A. S., & McCarthy, I. G. 2009, MNRAS, 400, 937

McGee, S. L., Balogh, M. L., Henderson, R. D. E., Wilman, D. J., Bower, R. G., Mulchaey, J. S., & Oemler, A. J. 2008, MNRAS, 664

McNamara, B. R. & Nulsen, P. E. J. 2007, ARA&A, 45, 117

Ménard, B., Kilbinger, M., & Scranton, R. 2009a, ArXiv e-prints

Ménard, B., Nestor, D., Turnshek, D., Quider, A., Richards, G., Chelouche, D., & Rao, S. 2008, MNRAS, 385, 1053

Ménard, B., Scranton, R., Fukugita, M., & Richards, G. 2009b, ArXiv e-prints

Montier, L. A. & Giard, M. 2005, A&A, 439, 35

Muller, S., Wu, S.-Y., Hsieh, B.-C., González, R. A., Loinard, L., Yee, H. K. C., & Gladders, M. D. 2008, ApJ, 680, 975

O'Donnell, J. E. 1994, ApJ, 422, 158

Parker, L. C., Hudson, M. J., Carlberg, R. G., & Hoekstra, H. 2005, ApJ, 634, 806

Pasquali, A., van den Bosch, F. C., Mo, H. J., Yang, X., & Somerville, R. 2009, MNRAS, 394, 38

Pei, Y. C. 1992, ApJ, 395, 130

Pfrommer, C., Springel, V., Enßlin, T. A., & Jubelgas, M. 2006, MNRAS, 367, 113

Prevot, M. L., Lequeux, J., Prevot, L., Maurice, E., & Rocca-Volmerange, B. 1984, A&A, 132, 389

Reiprich, T. H. & Böhringer, H. 2002, ApJ, 567, 716

Richards, G. T. & others. 2002, AJ, 123, 2945

Romani, R. W. & Maoz, D. 1992, ApJ, 386, 36

Rykoff, E. S., Evrard, A. E., McKay, T. A., Becker, M. R., Johnston, D. E., Koester, B. P., Nord, B., Rozo, E., Sheldon, E. S., Stanek, R., & Wechsler, R. H. 2008, MNRAS, 387, L28

Schlegel, D. J., Finkbeiner, D. P., & Davis, M. 1998, ApJ, 500, 525

Schneider, D. P. et al. 2007, AJ, 134, 102

Sheldon, E. S., Johnston, D. E., Masjedi, M., McKay, T. A., Blanton, M. R., Scranton, R., Wechsler, R. H., Koester, B. P., Hansen, S. M., Frieman, J. A., & Annis, J. 2007a, ArXiv e-prints

Sheldon, E. S., Johnston, D. E., Scranton, R., Koester, B. P., McKay, T. A., Oyaizu, H., Cunha, C., Lima, M., Lin, H., Frieman, J. A., Wechsler, R. H., Annis, J., Mandelbaum, R., Bahcall, N. A., & Fukugita, M. 2007b, ArXiv e-prints

Shen, S., Mo, H. J., White, S. D. M., Blanton, M. R., Kauffmann, G., Voges, W., Brinkmann, J., & Csabai, I. 2003, MNRAS, 343, 978

Spergel, D. N., Bean, R., Doré, O., Nolta, M. R., Bennett, C. L., Dunkley, J., Hinshaw, G., Jarosik, N., Komatsu, E., Page, L., Peiris, H. V., Verde, L., Halpern, M., Hill, R. S., Kogut, A., Limon, M., Meyer, S. S., Odegard, N., Tucker, G. S., Weiland, J. L., Wollack, E., & Wright, E. L. 2007, ApJS, 170, 377

Stickel, M., Klaas, U., Lemke, D., & Mattila, K. 2002, A&A, 383, 367

Tremonti, C. A., Moustakas, J., & Diamond-Stanic, A. M. 2007, ApJL, 663, L77

Tucker, D. L., Annis, J. T., Lin, H., Kent, S., Stoughton, C., Peoples, J., Allam, S. S., Mohr, J. J., Barkhouse, W. A., Ngeow, C., Alam, T., Beldica, C., Cai, D., Daues, G., Plante, R., Miller, C., Smith, C., & Suntzeff, N. B. 2007, in Astronomical Society of the Pacific Conference Series, Vol. 364, The Future of Photometric, Spectrophotometric and Polarimetric Standardization, ed. C. Sterken, 187–+

Vikhlinin, A., Markevitch, M., Murray, S. S., Jones, C., Forman, W., & Van Speybroeck, L. 2005, ApJ, 628, 655

Weingartner, J. C. & Draine, B. T. 2001, ApJ, 548, 296

Weinmann, S. M., van den Bosch, F. C., Yang, X., & Mo, H. J. 2006, MNRAS, 366, 2

Wilman, D. J., Balogh, M. L., Bower, R. G., Mulchaey, J. S., Oemler, A., Carlberg, R. G., Eke, V. R., Lewis, I., Morris, S. L., & Whitaker, R. J. 2005, MNRAS, 358, 88

Wise, M. W., O'Connell, R. W., Bregman, J. N., & Roberts, M. S. 1993, ApJ, 405, 94

Yang, X., Mo, H. J., van den Bosch, F. C., & Jing, Y. P. 2005, MNRAS, 356, 1293

Yang, X., Mo, H. J., van den Bosch, F. C., Pasquali, A., Li, C., & Barden, M. 2007, ApJ, 671, 153

Zackrisson, E., Micheva, G., & Orlin, G. 2009, ArXiv e-prints

Zibetti, S., White, S. D. M., Schneider, D. P., & Brinkmann, J. 2005, MNRAS, 358, 949

Zwicky, F. 1951, PASP, 63, 61